Author Manuscript

Author Manuscript

Author Manuscript

Author Manuscript

HHS Public Access

Author manuscript

Mol Cell. Author manuscript; available in PMC 2016 February 05.

Published in final edited form as:

Mol Cell. 2015 February 5; 57(3): 537–551. doi:10.1016/j.molcel.2015.01.002.

Erk2 phosphorylation of Drp1 promotes mitochondrial fission and MAPK-driven tumor growth

Jennifer A. Kashatus[1,4], **Aldo Nascimento**[1,4], **Lindsey J. Myers**[1], **Annie Sher**[2], **Frances L. Byrne**[3], **Kyle L. Hoehn**[3], **Christopher M. Counter**[2], and **David F. Kashatus**[1,*]

[1]Department of Microbiology, Immunology and Cancer Biology, University of Virginia Health System, Charlottesville, VA 22908

[2]Department of Pharmacology and Cancer Biology, Department of Radiation Oncology, Duke University Medical Center, Durham, NC 27710

[3]Department of Pharmacology, University of Virginia Health System, Charlottesville, VA 22908

Summary

Ras is mutated in up to 30% of cancers, including 90% of pancreatic ductal adenocarcinomas, causing it to be constitutively GTP-bound, and leading to activation of downstream effectors that promote a tumorigenic phenotype. As targeting Ras directly is difficult, there is a significant effort to understand the downstream biological processes that underlie its pro-tumorigenic activity. Here, we show that expression of oncogenic Ras or direct activation of the MAPK pathway leads to increased mitochondrial fragmentation and that blocking this phenotype, through knockdown of the mitochondrial fission-mediating GTPase Drp1, inhibits tumor growth. This fission is driven by Erk2-mediated phosphorylation of Drp1 on Serine 616 and both this phosphorylation and mitochondrial fragmentation are increased in human pancreatic cancer. Finally, this phosphorylation is required for Ras-associated mitochondrial fission and its inhibition is sufficient to block xenograft growth. Collectively, these data suggest mitochondrial fission may be a target for treating MAPK-driven malignancies.

Introduction

Mutations in *RAS* render the encoded small GTPase constitutively GTP-bound and active (Bos, 1989; Downward, 2003; Shields et al., 2000). In this state Ras stimulates downstream effectors that increase proliferation, block differentiation, reprogram metabolism and suppress apoptosis to drive oncogenesis (Shields et al., 2000). Despite this, direct

©2015 Published by Elsevier Inc.

*Correspondence: kashatus@virginia.edu.
[4]Co-first author

Publisher's Disclaimer: This is a PDF file of an unedited manuscript that has been accepted for publication. As a service to our customers we are providing this early version of the manuscript. The manuscript will undergo copyediting, typesetting, and review of the resulting proof before it is published in its final citable form. Please note that during the production process errors may be discovered which could affect the content, and all legal disclaimers that apply to the journal pertain.

Author Contributions J.A.K., A.N., L.J.M., A.S. & D.F.K. designed & performed all of the experiments. J.A.K., F.L.B, K.L.H., C.M.C. & D.F.K. discussed and interpreted experimental results. Manuscript was written by J.A.K. & D.F.K. with help from F.L.B, K.L.H. & C.M.C.

Author Manuscript Author Manuscript Author Manuscript Author Manuscript

pharmacological inhibition of Ras has been unsuccessful (Downward, 2003), so much attention has been focused on targeting critical Ras effector pathways, including the Raf, PI3K, and RalGEF pathways (Shields et al., 2000). Pharmacological inhibitors targeting the MAPK (Sebolt-Leopold and Herrera, 2004) and PI3K (Luo et al., 2003) pathways have been developed and shown to have anti-tumor activity, and there are numerous clinical trials testing such inhibitors for the treatment of a broad spectrum of cancers (Liu et al., 2009; Montagut and Settleman, 2009).

Several of the biological processes affected by Ras signaling, including apoptosis, proliferation, metabolic reprogramming and autophagy, are tightly linked to mitochondrial function and each of these processes can be affected by alterations in the balance of mitochondrial fusion and fission, suggesting that changes in mitochondrial morphology may underlie many of the phenotypes that drive tumorigenic growth (Liesa and Shirihai, 2013; Mitra, 2013; Youle and Karbowski, 2005). In support of this, mitochondrial fragmentation has been observed in tumor cells (Arismendi-Morillo, 2009; Inoue-Yamauchi and Oda, 2012; Rehman et al., 2012) and inhibition of mitochondrial fission decreases proliferation and increases apoptosis in models of lung cancer (Rehman et al., 2012) and colon cancer (Inoue-Yamauchi and Oda, 2012). Furthermore, the protein Survivin promotes increased glycolysis and tumorigenesis through increased mitochondrial fission (Hagenbuchner et al., 2013), mitochondrial fission is increased in invasive breast cancers and associated with increased metastatic potential (Zhao et al., 2013) and the mitochondrial fusion mediator Mfn2 is downregulated in gastric cancer (Zhang et al., 2013), and its knockdown promotes proliferation in B-cell lymphoma cells (Chen et al., 2014; Zhang et al., 2013). These studies support a link between mitochondrial fragmentation and tumor growth, but the mechanisms through which tumor cells promote this phenotype are not known and the physiological advantages gained from fragmentation have not been explored in detail.

Our previous work showed that the RalGEF-Ral pathway, an effector pathway downstream of oncogenic Ras, promotes mitochondrial fission during mitosis through mitochondrial recruitment and phosphorylation of the fission-mediating GTPase Drp1, suggesting a potential link between Ras and mitochondrial fission (Kashatus et al., 2011). As such, we hypothesized that altering the balance of mitochondrial fusion and fission might be a mechanism through which Ras promotes a number of the phenotypes associated with tumor progression and represent an attractive therapeutic target.

In support of this hypothesis, we find that expression of oncogenic Ras promotes a fragmented mitochondrial phenotype and that inhibition of this phenotype, through knockdown of Drp1, blocks tumor growth. Ras promotes this phenotype through activation of the MAPK pathway, as it is phenocopied through expression of activated cRaf and Mek1 and inhibited by treatment with the Mek inhibitor PD325901. Activation of the MAPK pathway promotes this phenotype, at least in part, through the direct phosphorylation of Serine 616 on Drp1 by Erk2 and levels of this phosphorylation are elevated in tissues and cells derived from pancreatic cancer patients. The importance of this phosphorylation is underscored by the fact that expression of wildtype, but not S616A, Drp1 reverses the mitochondrial elongation and loss of tumor growth observed upon knockdown of Drp1. These data suggest that induction of mitochondrial fission through phosphorylation of Drp1

Author Manuscript Author Manuscript Author Manuscript Author Manuscript

is a critical event in tumor growth driven by Ras or MAPK and that inhibitors targeting this process might have therapeutic potential for the treatment of tumors associated with the activation of these pathways.

Results

Expression of HRas^{G12V} promotes Drp1-dependent mitochondrial fragmentation

To determine whether activation of Ras affects mitochondrial dynamics, we expressed HRas^{G12V} in human embryonic kidney cells immortalized with SV-40 large and small T antigens and hTert (HEK-TtH) (Hahn et al., 1999) and analyzed the mitochondrial morphology by staining with MitoTracker Red (Figure 1A, 1B). Expression of HRas^{G12V} promoted a shift in mitochondrial morphology, with greater than 80% of cells exhibiting a fragmented morphology compared to less than 25% of control cells (Figure 1A, 1C).

Mitochondrial morphology is determined by a balance of the processes of fusion and fission, which are mediated by large GTPases of the dynamin family (Westermann, 2010). To determine the importance of mitochondrial fission for the shift towards a fragmented mitochondrial phenotype, we used shRNA to knock down expression of the fission-mediating GTPase Drp1 (Figure 1B). Expression of the Drp1 shRNA reversed the fragmented phenotype and caused the cells to exhibit an interconnected phenotype (Figure 1A, 1C). This change was not associated with major changes in mitochondrial function, as the basal oxygen consumption rate was unchanged following knockdown of Drp1 (Figure S1A). Likewise, there was no decrease in membrane potential, as measured by TMRE loading (Figure S1B). The only difference observed following knockdown of Drp1 was an increase in mitochondrial mass (Figure S1C) along with an increase in spare respiratory capacity (Figure S1A).

To further analyze the effects of Ras expression on mitochondrial dynamics, we employed a mitochondria-targeted photoactivatable Green Fluorescent Protein (mt-PA-GFP) (Karbowski et al., 2004). Activation of mt-PA-GFP in vector control cells led to a rapid diffusion of the fluorescent signal throughout the entire mitochondrial network (Figure 1D). In the HRas^{G12V}-expressing cells, on the other hand, the GFP signal did not readily diffuse despite some observable fusion events. These data indicate that Ras-induced mitochondrial fragmentation requires Drp1, but that a concomitant decrease in fusion activity cannot be ruled out. Furthermore, the data are consistent with the previously observed association between oncogenic transformation and mitochondrial fragmentation, and suggest a potential mechanistic link between Ras activity and altered mitochondrial morphology.

Ras-driven tumor growth requires Drp1

HEK-TtH cells expressing HRas^{G12V} are able to form tumors in immunocompromised mice (Hamad et al., 2002), making them a useful model to study Ras-mediated tumorigenesis. To test whether mitochondrial fragmentation is important for tumor growth, we injected the HEK-TtH cells expressing HRas^{G12V} and either scramble or Drp1 shRNA subcutaneously (Figure 1E) and found that expression of Drp1 shRNA caused a significant reduction in tumor volume ($p=0.00749$) and tumor weight ($p=0.00242$) (Figure 1E–1G). These results

Author Manuscript Author Manuscript Author Manuscript Author Manuscript

were recapitulated by expression of the dominant-negative Drp1^{K38A} (Pitts et al., 2004) (Figure S1D–G), suggesting that the loss in tumor growth is not an off-target effect of the Drp1 shRNA. These data are consistent with a previous report that over-expression of the fusion GTPase Mfn2 or intratumoral injection of the Drp1 inhibitor Mdivi-1 can inhibit the tumorigenic growth of a lung adenocarcinoma cell line (Rehman et al., 2012) and suggest that Drp1 is a potential therapeutic target in tumors expressing oncogenic Ras.

Erk2 is a Drp1 kinase

We next sought to explore the mechanism through which Ras expression changes mitochondrial morphology. The observed fragmented phenotype is dependent on Drp1, consistent with an induction of fission activity. Mitochondrial fission is regulated through recruitment of Drp1 to mitochondrial membranes, its assembly into a ring structure and the constriction of that ring (Westermann, 2010). These processes are regulated by specific protein-protein interactions between Drp1 and mitochondrial membrane proteins, as well as post-translational modifications, including phosphorylation of S616, which promotes Drp1 activity (Taguchi et al., 2007), and S637 which inhibits its activity (Chang and Blackstone, 2007). We previously showed that the GTPase RalA and its effector RalBP1 drive mitochondrial fission during mitosis by promoting Cdk1-mediated phosphorylation of S616 and recruitment to the mitochondrial outer membrane (Kashatus et al., 2011). While this pathway is one potential mechanism through which activation of Ras promotes mitochondrial fragmentation, the persistence of the fragmentation throughout all phases of the cell cycle observed in HRas^{G12V}-expressing cells (Figure 1A) led us to speculate that Ras signals to the mitochondrial fission machinery through additional routes. Interestingly, our analyses of the sequences surrounding S616 revealed that it represents a perfect consensus sequence for phosphorylation by Erk2 (Carlson et al., 2011) and that this site is conserved throughout vertebrate evolution (Figure 2A). Furthermore, Erk activity has previously been shown to promote mitochondrial fission, and *in vitro* kinase assays using recombinant Erk1 have suggested that Erk1 may directly phosphorylate Drp1 (Gan et al., 2014; Yu et al., 2011). As the MAPK pathway is a key effector pathway downstream of activated Ras (Shields et al., 2000), phosphorylation of Drp1 by Erk2 would provide an additional potential mechanism for the Ras-induced mitochondrial fragmentation we observe.

To test whether Erk2 phosphorylates Drp1, we incubated recombinant, constitutively active Erk2^{R67S} (Levin-Salomon et al., 2008) and γ^{32}P-ATP with recombinant GST or GST fused to the C-terminal 219 amino acids of Drp1 (Drp1$^{518–736}$) in either the wildtype or S616A configuration. Erk2 phosphorylated wildtype Drp1, but not the S616A mutant or GST alone (Figure 2B). We repeated the experiment using non-radioactive ATP and an S616 phospho-specific antibody, finding that only the combination of activate Erk2 and wildtype Drp1 resulted in a detectable signal (Figure 2C). These experiments confirm that Erk2 is a kinase for S616 on Drp1 and provide a potential mechanism through which Ras promotes mitochondrial fission.

Author Manuscript Author Manuscript Author Manuscript Author Manuscript

Drp1 S616 is phosphorylated following activation of the MAPK pathway

To determine whether Erk2 phosphorylation of Drp1 occurs in a more physiological setting, we used gain- and loss-of-function approaches. First, we incubated HEK-TtH cells overnight in the absence of serum and the presence of the Mek inhibitor PD325901 to inhibit Erk signaling (Sebolt-Leopold and Herrera, 2004). Following the incubation, we replaced the media with fresh media containing 10% fetal bovine serum and evaluated the phosphorylation of both Erk and Drp1 over an 8-hour timecourse. Addition of serum led to an increase in phospho-Erk1/2 (T202/Y204), indicating activation of the MAPK pathway, closely followed by an increase in S616-phosphorylated Drp1 (Figure 2D). Conversely, when we treated cells grown in serum with increasing concentrations of PD325901, we observed a dose-dependent decrease in Drp1 phosphorylation that closely tracked the inhibition of Erk phosphorylation (Figure 2E). Identical effects were observed when we treated HEK-TtH cells stably expressing $HRas^{G12V}$, suggesting that the serum-induced effects are through Ras and its downstream signaling pathways (Figure 2F). To more specifically test the ability of the MAPK pathway to promote Drp1 phosphorylation, we transiently transfected serum-starved HEK-TtH cells with a constitutively active mutant of c-Raf (Raf-22W) (Stanton et al., 1989). Raf-22W expression led to increased Erk phosphorylation as well as increased phosphorylation of Drp1 (Figure 2G). To rule out the possibility that this is peculiar to our HEK-TtH system, we repeated this experiment in HeLa cells and confirmed that expression of Raf-22W led to an increase in both Erk and Drp1 phosphorylation (Figure 2H). Further, when we transfected cells simultaneously treated with PD325901, we observed a near complete loss of both Erk and Drp1 phosphorylation, indicating that Raf-induced Drp1 phosphorylation is dependent on Mek activity (Figure 2H, lanes 4–6). Notably, neither inhibition of Mek activity in the presence of serum or $HRas^{G12V}$, nor expression of Raf-22W, led to changes in the levels of the fusion proteins Mfn1, Mfn2 and Opa1 (Figure S2A,B,C).

The Mek dependence of S616 phosphorylation led us to test whether expression of an activated mutant of Mek also promotes Drp1 phosphorylation. As with Raf-22W, transient expression of an activated Mek1 mutant (Mek-DD) (Brunet et al., 1994) led to an increase in Drp1 phosphorylation in both HEK-TtH (Figure 2I) and HeLa cells (Figure 2J) and this increase was abolished by treatment with PD325901 (Figure 2J, lanes 7–12).

These data indicate that activation of the MAPK pathway through several routes leads to a Mek-dependent increase in Drp1 phosphorylation and, with the *in vitro* data, are consistent with the hypothesis that Ras activation of the MAPK pathway promotes phosphorylation of Drp1 S616 by Erk2.

Activation of MAPK signaling induces mitochondrial fragmentation

As phosphorylation of Drp1 S616 promotes mitochondrial fission, we evaluated whether activation of the MAPK pathway is necessary to induce the fragmented mitochondrial phenotype induced by oncogenic $HRas^{G12V}$. As such, we treated HEK-TtH cells expressing $HRas^{G12V}$ with DMSO or PD325901 and visualized the mitochondrial morphology. Treatment with the inhibitor led to a complete reversal of the Ras-induced mitochondrial

Author Manuscript Author Manuscript Author Manuscript Author Manuscript

phenotype, with >80% of the drug-treated cells exhibiting an interconnected phenotype, compared with <5% of the vehicle-treated cells (Figure 3A,B).

These results indicate that the MAPK pathway is *necessary* for Ras-induced mitochondrial fragmentation. To test whether the pathway is *sufficient* for fragmentation, we utilized the constitutively activated mutants of Raf and Mek. Transient expression Raf-22W or Mek-DD completely phenocopied the mitochondrial fragmentation observed following expression of activated Ras and this fragmentation was completely reversed by treatment with PD325901 (Figure 3C–3F). These data suggest that Ras-mediated activation of the MAPK pathway is both necessary and sufficient to promote a fragmented mitochondrial phenotype. Thus, while the RalGEF pathway promotes mitochondrial fission during mitosis (Kashatus et al., 2011), the MAPK plays a dominant role in promoting the fragmented phenotype in the context of constitutive Ras activity.

Drp1 is phosphorylated in pancreatic cancer cell lines

As exogenous expression of oncogenic Ras, or activation of MAPK signaling, promotes phosphorylation of Drp1 and mitochondrial fragmentation, we examined whether the *endogenous* activation of these pathways observed in pancreatic cancer promotes the same phenotype. Thus, we analyzed the levels of phosphorylated Drp1 and the mitochondrial morphology in a series of patient-derived, KRas-mutant pancreatic cancer cell lines: Capan-1, Capan-2, CFPAC-1, PANC-1, L3.6PL, MPanc96 and VMP 608t (Bruns et al., 1999; Deer et al., 2010; Moore et al., 2001; Stokes et al., 2011) and one cell line with wildtype Ras: BxPC-3 (Diep et al., 2011). Each of the cell lines had detectable levels of S616-phosphorylated Drp1 by immunoblot (Figure 4A). Treatment of MPanc-96 cells with PD325901 led to a dose-dependent decrease in Drp1 S616 phosphorylation that temporally followed a decrease in Erk phosphorylation, suggesting that the MAPK pathway contributes to the phosphorylation (Figure 4B,C). Like HEK-TtH cells, treatment with the inhibitor had no observable effect on the levels of fusion proteins (Figure S3A). Additionally, the mitochondrial morphology of each of the cell lines exhibited a highly fragmented phenotype (Figure 4D and S3B), similar to what we observed in HEK-TtH cells expressing $HRas^{G12V}$.

To determine if Mek-dependent phosphorylation of Drp1 is important for the observed fragmented mitochondrial phenotype, MPanc96 cells were treated with PD325901 for 24 hrs and the mitochondrial morphology analyzed. Consistent with the data from HEK-TtH cells, inhibition of Mek led to a reversal of the fragmented phenotype, with 50% of the PD325901-treated cells exhibiting an interconnected phenotype, compared to less than 5% of controls (Figure 4E).

Stable knockdown of Drp1 inhibits pancreatic tumor growth

To determine the importance of mitochondrial fission for tumor growth, we stably knocked down Drp1 in BxPC3 cells, which have wildtype Ras but high levels of MAPK activity and rely on MAPK signaling for their tumorigenic growth (Diep et al., 2011; Holcomb et al., 2008). Knockdown of Drp1 had a significant effect on BxPC3 tumor growth, with a significant delay observed in cells expressing the Drp1 shRNA compared with the scramble controls (Figure 4F,G). Furthermore, the size of the tumors that arose from the Drp1

Author Manuscript Author Manuscript Author Manuscript Author Manuscript

knockdown was variable, and immunoblots of the tumor lysates indicated that the larger tumors expressed higher levels of Drp1 (Figure 4H). These data suggest that there is selective pressure against knockdown of Drp1 and that cells with higher basal levels have a distinct growth advantage *in vivo*, lending support to the idea that Erk-induced Drp1 activity is important for tumor growth.

We performed the same analysis with two additional pancreatic cancer cell lines, L3.6PL and MPanc96, but observed no effect on tumor growth following knockdown of Drp1 (Figure S3C, S3D). However, like the BxPC3 cells, analysis of the tumors revealed re-expression of Drp1 in the tumors that arose (Figure S3E, S3F), suggesting selective pressure against Drp1 knockdown and indicating that alternative methods of inhibition will be required to test the requirement of Drp1 more broadly.

Drp1 is phosphorylated in pancreatic tumor specimens

We also analyzed Drp1 phosphorylation by direct immunohistochemical staining of patient-derived pancreatic cancer specimens, as the majority of pancreatic cancers have mutations in KRAS and/or constitutive MAPK pathway activation (Bos, 1989). Serial sections were cut from 12 formalin-fixed, paraffin-embedded (FFPE) surgically resected pancreatic ductal adenocarcinomas, then stained using hematoxylin and eosin (H&E) as well as antibodies specific for S616-phosphorylated Drp1 and T202/Y204-phosphorylated Erk1/2, with representative images from 6 of the tumors shown in Figure 5A. The specificity of the Drp1 antibody was confirmed by staining sections cut from FFPE cell pellets of HEK-TtH cells expressing $HRas^{G12V}$ and Drp1 shRNA in addition to shRNA-resistant Drp1 or $Drp1^{S616A}$ (Figure S4). We detected high to moderate levels (2+/3+) of phospho-Erk staining in a large percentage of the tumor area, but not the surrounding normal tissue, for 10 of the 12 sections (Figure 5B). We also observed low to moderate (1+/2+) Drp1 phospho-S616 staining in 11 of the 12 tumors. Consistent with our hypothesis that Erk is upstream of Drp1 phosphorylation, 7 of 12 tumors exhibited a high degree of colocalization between the phospho-Erk and phospho-Drp1 staining while an additional 2 tumors exhibited partial colocalization. Of the remaining 3 tumors, two exhibited non-overlapping phospho-Drp1 and phospho-Erk while one was negative for both (Figure 5B). To see if these tumors also exhibited mitochondrial fragmentation, we stained additional sections of two tumors with a fluorescently conjugated antibody that recognizes mitochondria (MTC02). Mitochondria in these sections exhibited a high degree of fragmentation (Figure 5C) while cells in areas outside of the tumor boundary exhibited an intermediate mix of mitochondrial morphologies (not shown). Collectively, these data suggest that activation of the MAPK pathway leads to an increase in mitochondrial fission that occurs, at least in part, through Erk2-mediated phosphorylation of Drp1 and that this regulation occurs in human pancreatic cancer.

Drp1 S616 phosphorylation is required for Ras-induced mitochondrial fission and tumor growth

To determine the importance of Drp1 phosphorylation for the phenotypes we have observed, we expressed wildtype or S616A, shRNA-resistant Drp1 in the HEK-TtH cells expressing $HRas^{G12V}$ and Drp1 shRNA. Re-expression of the wildtype, but not the SA mutant restored the levels of Drp1 phosphorylation (Figure 6A). Further, expression of wildtype Drp1, but

Author Manuscript Author Manuscript Author Manuscript Author Manuscript

not the mutant, completely restored the highly fragmented phenotype of the $HRas^{G12V}$-expressing cells lost upon knockdown of Drp1 (Figure 6B,C). To test the hypothesis that phosphorylation of Drp1 S616 is important for tumor growth, we injected these cells into mice. Knockdown of Drp1 led to a loss of tumor growth and re-expression of wildtype Drp1, but not the SA mutant, restored tumor growth to the levels observed in the scramble control cells (Figure 6D–E). These data link the effects of MAPK activation on mitochondrial morphology to the biological requirement of Drp1 for tumor growth and underscore the direct physiological relevance of the Erk2-mediated phosphorylation of Drp1 that we observe.

Discussion

The MAPK pathway is activated in a large percentage of human tumors, but the direct targets of this pathway most critical for its pro-tumorigenic effects are not known. We have described a substrate of Erk2, the mitochondrial fission GTPase Drp1, which is critically important for tumor growth. Furthermore, we show that by inhibiting this phosphorylation, but not changing any of the other downstream targets of Erk, we can alter the mitochondrial phenotype of Ras-expressing cells and prevent tumor growth.

Mitochondrial dynamics have been known to play an important role in a number of human diseases including obesity and type 2 diabetes (Yoon et al., 2011), Parkinson's disease (Lim et al., 2012) and Alzheimer's disease (Su et al., 2010), but the role of mitochondrial fusion and fission in malignancy has only recently begun to be explored (Qian et al., 2013). Consistent with our findings, the majority of studies that have explored mitochondrial morphology in tumor cells support a pro-tumorigenic role for mitochondrial fission (Arismendi-Morillo, 2009; Chen et al., 2014; Hagenbuchner et al., 2013; Inoue-Yamauchi and Oda, 2012; Rehman et al., 2012; Zhang et al., 2013; Zhao et al., 2013). Despite this, the molecular mechanisms through which oncogenic signaling pathways can alter mitochondrial dynamics have not been well defined. Our previous work defined a pathway through which the small GTPase and important Ras effector protein RalA, along with its effector RalBP1, promotes mitochondrial fission during mitosis by promoting the recruitment of Drp1 to the mitochondria and enabling its phosphorylation by Cdk1 (Kashatus et al., 2011). The work presented here identifies an additional pathway downstream of Ras to promote Drp1 activity and mitochondrial fragmentation and underscores the importance of mitochondrial fragmentation for Ras- and MAPK-driven tumor growth. These studies provide the molecular mechanism that underlies the change in mitochondrial morphology we observe in pancreatic cancer cell lines and, potentially, the changes observed by others in a number of different cancer cell lines (Inoue-Yamauchi and Oda, 2012). Furthermore, this study demonstrates the importance of this morphological change in a genetically-defined model system of Ras-driven tumor growth.

There are a number of physiological mechanisms that could potentially explain the loss tumor growth observed upon inhibition of Drp1, as the regulation of mitochondrial fusion and fission has been shown to play a role in several physiological processes whose dysregulation are classical "hallmarks" of human cancer (Hanahan and Weinberg, 2011), including apoptosis (Sheridan and Martin, 2010), and proliferation (Mitra et al., 2009; Qian

Author Manuscript Author Manuscript Author Manuscript Author Manuscript

et al., 2012). Our results, however, suggest that inhibition of Drp1 does not block tumor growth through direct effects on either proliferation or apoptosis (Figure S5A,B). The loss of major tumor suppressor pathways, through expression of SV-40 large and small T antigens in the HEK-TtH cells, may explain why we do not observe the previously documented effects on proliferation and survival and suggests that inhibition of Drp1 may be an effective therapeutic option even in tumors that have disabled their apoptotic and growth arrest capabilities.

The rapid proliferation of tumor cells requires a large increase in the production of molecular building blocks and tumors achieve this through increased uptake of both glucose and glutamine, which are used for both ATP generation and biosynthesis (Diaz-Ruiz et al., 2009; Ferreira, 2010; Vander Heiden et al., 2009; Warburg, 1956), and through increased autophagy, which can provide biosynthetic precursors and contribute to the metabolic reprogramming (Lozy and Karantza, 2012; Rosenfeldt and Ryan, 2011). Indeed, Ras-driven tumors in particular exhibit high levels of mitophagy (Kim et al., 2011) and a number of groups over the past several years have shown that autophagy plays an essential role in tumors driven by oncogenic Ras or mutant BRaf (Guo et al., 2011; Lock et al., 2011; Rao et al., 2014; Rosenfeldt et al., 2013; Son et al., 2013; Strohecker et al., 2013). We observe a marked increase in mitochondrial mass and mitochondrial protein levels following knockdown of Drp1 in cells expressing $HRas^{G12V}$ (Figure S1C, S5C). Furthermore, the increased mitochondrial protein levels of Drp1 knockdown cells are unaffected by inhibition of autophagy, suggesting that mitophagy has already been inhibited in these cells (Figure S5D). However, we have no evidence that the inhibition of tumor growth we observe is due to a loss of mitophagy. We do, however, consistently observe a phenotypic difference in the color of the tumors that arise following Drp1 inhibition that suggests a decrease in tumor vasculature (Figures 1F, S1F, S5E, S5F). Further, our preliminary analysis indicates that knockdown of Drp1 in HEK-TtH $HRas^{G12V}$ cells results in lower levels of VEGF mRNA and decreased tumor vasculature as measured by staining for CD31 (Figure S5G, S5H). We speculate that MAPK-induced mitochondrial fission may promote the activation of pro-angiogenic signaling pathways, which are known to be sensitive to mitochondria-derived reactive oxygen species (Ushio-Fukai and Nakamura, 2008; Xia et al., 2007). Further analysis of this phenomenon is warranted to determine whether this regulation plays a significant role in the observed effects.

These potential mechanisms (i.e. – proliferation, apoptosis, metabolism, mitophagy, angiogenesis, etc.) through which mitochondrial fission promotes tumor growth are not mutually exclusive, and changes in mitochondrial morphology may function through different combinations of these and other mechanisms in different types of tumors or in response to different stromal environments. It will be important to test these potential mechanisms in a variety of different model systems in order to fully explore the possibility of mitochondrial fission inhibition as a therapeutic approach to cancer treatment.

In conclusion, we show that the MAPK regulation of mitochondrial fission through phosphorylation of the fission-mediating GTPase Drp1 is essential in a model of Ras-driven tumor growth. Furthermore, identification of this pathway provides a mechanistic link between mutations in *RAS* and several physiological changes characteristic of Ras-driven

Author Manuscript Author Manuscript Author Manuscript Author Manuscript

tumors and potentially offers an avenue of therapeutic intervention for the treatment of a wide variety of human cancers.

Experimental Procedures

Cell culture

HEK-TtH cells have been described previously (Hahn et al., 1999; Lim et al., 2005). HEK-TtH, HeLa, CFPac and Panc-1 cells were maintained in Dulbecco's Modified Eagle Medium (DMEM – Life Technologies) supplemented with 10% Fetal Bovine Serum (FBS – Life Technologies). VMP 608t, BxPC3, L3.6PL and MPanc96 were maintained in RPMI medium (Life Technologies) supplemented with 10% FBS. Capan-1 and Capan-2 were maintained in Iscove's Modified Dulbecco's Medium (IMDM – Life Technologies) supplemented with 10% FBS.

Protein analysis

Whole cell lysates were prepared in RIPA buffer and equivalent protein amounts (generally 50 or 100μg) were resolved by SDS-Page. Alternatively, equal cell numbers were lysed directly in SDS-Page sample loading buffer and resolved by SDS-Page. Gels were transferred to PVDF membranes and immunoblotted with the indicated antibodies.

Xenografts

2.5×10^6 (Figure 1, S1), 5×10^6 (Figure 4, S3) or 1×10^7 (Figure 6) cells were resuspended in phosphate buffered saline (PBS), mixed 1:1 with Matrigel and injected subcutaneously into the flanks of SCID/beige (Charles River Laboratory), or Athymic Nude-*FoxN1*^{nu} mice (Harlan). Tumor volumes were determined twice per week and calculated as (length × width^2)π/6. Mice were sacrificed when the tumors reached 1000mm^3 or the mice exhibited signs of moribundity, at which point tumors were removed and weighed. Tumors were halved at harvest and formalin-fixed paraffin-embedded or flash frozen. Experiments were approved by the Duke University Institutional Animal Care and Use Committee and the University of Virginia Animal Care and Use Committee.

Mito-PAGFP assay

HEK-TtH or HEK-TtH HRas^{G12V} cells were plated on glass bottom microwell dishes (MatTek) and transiently co-transfected with 1ug each pDsRed2-Mito and mito-PAGFP. The next day, cells were imaged on an LSM700 confocal microscope (Zeiss) equipped with a 63× oil objective, heated stage and 5% CO_2 incubation. Positively transfected cells were identified as containing red fluorescent mitochondria. A 4μm-wide ROI strip was selected and activated by a single pulse 405-nm laser. Red and green fluorescent Z-stacks (10 slices, 0.7μm each) were acquired before and immediately following activation, then every 15 minutes for 1 hour. Images show z-stack reconstruction of representative cells at each timepoint. 5–10 cells were assayed per condition.

Author Manuscript Author Manuscript Author Manuscript Author Manuscript

Immunofluorescence

The described HEK-TtH, HeLa or pancreatic cancer cell lines were plated on glass microslides the previous day, then mitochondria were visualized by one of the following methods: (1) Cells were treated with 100nM MitoTracker Red CMXRos (Life Technologies) for 30 minutes, fixed, permeabilized and mounted immediately in Prolong Gold antifade reagent with DAPI (Life Technologies); (2) Cells were fixed, permeabilized and incubated with α-Tom20 primary antibody in conjunction with an α-rabbit Alexa-488 secondary antibody (Life Technologies); (3) Cells were engineered to stably express mitochondria-targeted YFP (BD Biosciences). A Zeiss LSM 700 confocal microscope with 63× oil objective was used for imaging. A cell was judged to have fragmented mitochondria if fewer than 25% of the mitochondria visible in the cell had a length 5 times its width and highly interconnected if greater than 75% of the mitochondria had a length 5 times its width. For quantitation, greater than 50 cells per cell type were blindly analyzed by 3–5 people.

In Vitro Kinase Assays

Recombinant GST-Drp1$^{518–736}$, GST-Drp1$^{518–736,S616A}$ and GST-Erk2^{R67S} were purified from bacteria using glutathione-sepharose-4B (GE) and eluted with 15mM glutathione (Sigma) in elution buffer. Proteins were dialyzed overnight in 2L elution buffer and concentrated with an Amicon Ultra 10K centrifugal filter device (Millipore). In vitro kinase reactions were performed as described (Levin-Salomon et al., 2008). Briefly, 500ng GST-Erk2^{R67S} was incubated with 500ng of either GST, GST-Drp1$^{518–736}$, or GST-Drp1$^{518–736,S616A}$ in 25μl 1× Kinase Buffer, incubated for 30 minutes at 30°C then terminated with the addition of 25μl SDS-Page sample loading buffer and resolved by SDS-Page followed by either autoradiography (Hot) or immunoblot (Cold).

Immunohistochemistry

12 HIPAA de-identified pancreatic carcinoma specimens, present as formalin-fixed, paraffin-embedded blocks, were obtained from the University of Virginia Biorepository and Tissue Research Facility (BTRF). Tissue sections were cut from each block at 4μm thick intervals. Antigen retrieval and deparaffinization were performed in PT Link (Dako, Glostrup, Denmark) using low pH for p-DRP1 and high pH for p-ERK, EnVision FLEX Target Retrieval Solution (Dako) for 20 min at 97°C. Immunohistochemistry was performed on a robotic platform (Autostainer, Dako). Endogenous peroxidases were blocked with peroxidase and alkaline Phosphatase blocking reagent (Dako) before incubating the sections with p-Drp1 at 1:25 dilution for 60 minutes and p-Erk at 1:200 dilution for 30 minutes at room temperature. Antigen–antibody complex was detected using Envision™ Dual Link (Dako) followed by incubation with 3,3′-diaminobenzidine tetrahydrochloride (DAB+) chromogen (Dako). All slides were subsequently counterstained with hematoxylin then dehydrated, cleared and mounted for assessment. Immunofluorescence on formalin-fixed paraffin-embedded (FFPE) sections was performed as previously described (Wang et al., 2011) on 2 of the 12 HIPAA de-identified pancreatic carcinoma specimens. Briefly, FFPE sections were deparaffinized and antigen-retrieved, washed and blocked then incubated with anti-Mitochondria antibody, clone 113–1, Cy3 conjugate (EMD Millipore) overnight. Slides were incubated with $CuSO_4$ to reduce autofluorescence and mounted with Prolong Gold

Author Manuscript Author Manuscript Author Manuscript Author Manuscript

antifade reagent with DAPI. Images were taken with a Zeiss LSM 710 Multiphoton microscope with a 20× (NA 0.8) or 63× (NA 1.4) objective.

Supplementary Material

Refer to Web version on PubMed Central for supplementary material.

Acknowledgments

We thank M. Dunlap-Brown and the University of Virginia Molecular Assessments and Preclinical Studies Core Facility for assistance with xenografts; P. Pramoonjago, C. Rumpel and the University of Virginia Biorepository and Tissue Research Facility for tumor specimens and immunohistochemical analysis; S. Dustin-Hess and C. Moskaluk for assistance with pathology; M. Solga for assistance with flow cytometry; T. Parsons, T. Bauer and K. Kelly for pancreatic cancer cell lines; D. Brady for recombinant Erk2 and pGEX-Mek-DD and useful discussions; R. Youle for mito-PAGFP; J. Cross for VEGF primers and technical assistance; A. Bouton, M. Smith, D. Gioeli and M. Weber for discussion. This work was aided by Grant #IRG 81-001-26 from the American Cancer Society to D.F.K.

References

Arismendi-Morillo G. Electron microscopy morphology of the mitochondrial network in human cancer. Int J Biochem Cell Biol. 2009; 41:2062–2068. [PubMed: 19703662]

Bos JL. ras oncogenes in human cancer: a review. Cancer Res. 1989; 49:4682–4689. [PubMed: 2547513]

Brunet A, Pagès G, Pouysségur J. Constitutively active mutants of MAP kinase kinase (MEK1) induce growth factor-relaxation and oncogenicity when expressed in fibroblasts. Oncogene. 1994; 9:3379–3387. [PubMed: 7936666]

Bruns CJ, Harbison MT, Kuniyasu H, Eue I, Fidler IJ. In vivo selection and characterization of metastatic variants from human pancreatic adenocarcinoma by using orthotopic implantation in nude mice. Neoplasia. 1999; 1:50–62. [PubMed: 10935470]

Carlson SM, Chouinard CR, Labadorf A, Lam CJ, Schmelzle K, Fraenkel E, White FM. Large-scale discovery of ERK2 substrates identifies ERK-mediated transcriptional regulation by ETV3. Sci Signal. 2011; 4:rs11. [PubMed: 22028470]

Chang CR, Blackstone C. Cyclic AMP-dependent protein kinase phosphorylation of Drp1 regulates its GTPase activity and mitochondrial morphology. J Biol Chem. 2007; 282:21583–21587. [PubMed: 17553808]

Chen KH, Dasgupta A, Ding J, Indig FE, Ghosh P, Longo DL. Role of mitofusin 2 (Mfn2) in controlling cellular proliferation. Faseb J. 2014; 28:382–394. [PubMed: 24081906]

Deer EL, González-Hernández J, Coursen JD, Shea JE, Ngatia J, Scaife CL, Firpo MA, Mulvihill SJ. Phenotype and Genotype of Pancreatic Cancer Cell Lines. Pancreas. 2010; 39:425–435. [PubMed: 20418756]

Diaz-Ruiz R, Uribe-Carvajal S, Devin A, Rigoulet M. Tumor cell energy metabolism and its common features with yeast metabolism. Biochim Biophys Acta. 2009; 1796:252–265. [PubMed: 19682552]

Diep CH, Munoz RM, Choudhary A, Hoff Von DD, Han H. Synergistic effect between erlotinib and MEK inhibitors in KRAS wild-type human pancreatic cancer cells. Clin Cancer Res. 2011; 17:2744–2756. [PubMed: 21385921]

Downward J. Targeting RAS signalling pathways in cancer therapy. Nat Rev Cancer. 2003; 3:11–22. [PubMed: 12509763]

Ferreira LMR. Cancer metabolism: the Warburg effect today. Exp Mol Pathol. 2010; 89:372–380. [PubMed: 20804748]

Gan X, Huang S, Wu L, Wang Y, Hu G, Li G, Zhang H, Yu H, Swerdlow RH, Chen JX, et al. Inhibition of ERK-DLP1 signaling and mitochondrial division alleviates mitochondrial dysfunction in Alzheimer's disease cybrid cell. Biochim Biophys Acta. 2014; 1842:220–231. [PubMed: 24252614]

Author Manuscript Author Manuscript Author Manuscript Author Manuscript

Guo JY, Chen HY, Mathew R, Fan J, Strohecker AM, Karsli-Uzunbas G, Kamphorst JJ, Chen G, Lemons JMS, Karantza V, et al. Activated Ras requires autophagy to maintain oxidative metabolism and tumorigenesis. Gene Dev. 2011; 25:460–470. [PubMed: 21317241]

Hagenbuchner J, Kuznetsov AV, Obexer P, Ausserlechner MJ. BIRC5/Survivin enhances aerobic glycolysis and drug resistance by altered regulation of the mitochondrial fusion/fission machinery. Oncogene. 2013; 32:4748–4757. [PubMed: 23146905]

Hahn WC, Counter CM, Lundberg AS, Beijersbergen RL, Brooks MW, Weinberg RA. Creation of human tumour cells with defined genetic elements. Nature. 1999; 400:464–468. [PubMed: 10440377]

Hamad NM, Elconin JH, Karnoub AE, Bai W, Rich JN, Abraham RT, Der CJ, Counter CM. Distinct requirements for Ras oncogenesis in human versus mouse cells. Gene Dev. 2002; 16:2045–2057. [PubMed: 12183360]

Hanahan D, Weinberg RA. Hallmarks of cancer: the next generation. Cell. 2011; 144:646–674. [PubMed: 21376230]

Holcomb B, Yip-Schneider MT, Matos JM, Dixon J, Kennard J, Mahomed J, Shanmugam R, Sebolt-Leopold J, Schmidt CM. Pancreatic cancer cell genetics and signaling response to treatment correlate with efficacy of gemcitabine-based molecular targeting strategies. J Gastrointest Surg. 2008; 12:288–296. [PubMed: 18049840]

Inoue-Yamauchi A, Oda H. Depletion of mitochondrial fission factor DRP1 causes increased apoptosis in human colon cancer cells. Biochem Bioph Res Co. 2012; 421:81–85.

Karbowski M, Arnoult D, Chen H, Chan DC, Smith CL, Youle RJ. Quantitation of mitochondrial dynamics by photolabeling of individual organelles shows that mitochondrial fusion is blocked during the Bax activation phase of apoptosis. J Cell Biol. 2004; 164:493–499. [PubMed: 14769861]

Kashatus DF, Lim KH, Brady DC, Pershing NLK, Cox AD, Counter CM. RALA and RALBP1 regulate mitochondrial fission at mitosis. Nat Cell Biol. 2011; 13:1108–1115. [PubMed: 21822277]

Kim JH, Kim HY, Lee YK, Yoon YS, Xu WG, Yoon JK, Choi SE, Ko YG, Kim MJ, Lee SJ, et al. Involvement of mitophagy in oncogenic K-Ras-induced transformation: overcoming a cellular energy deficit from glucose deficiency. Autophagy. 2011; 7:1187–1198. [PubMed: 21738012]

Levin-Salomon V, Kogan K, Ahn NG, Livnah O, Engelberg D. Isolation of intrinsically active (MEK-independent) variants of the ERK family of mitogen-activated protein (MAP) kinases. J Biol Chem. 2008; 283:34500–34510. [PubMed: 18829462]

Liesa M, Shirihai OS. Mitochondrial dynamics in the regulation of nutrient utilization and energy expenditure. Cell Metab. 2013; 17:491–506. [PubMed: 23562075]

Lim KL, Ng XH, Grace LGY, Yao TP. Mitochondrial dynamics and Parkinson's disease: focus on parkin. Antioxid Redox Sign. 2012; 16:935–949.

Lim KH, Baines AT, Fiordalisi JJ, Shipitsin M, Feig LA, Cox AD, Der CJ, Counter CM. Activation of RalA is critical for Ras-induced tumorigenesis of human cells. Cancer Cell. 2005; 7:533–545. [PubMed: 15950903]

Liu P, Cheng H, Roberts TM, Zhao JJ. Targeting the phosphoinositide 3-kinase pathway in cancer. Nat Rev Drug Discov. 2009; 8:627–644. [PubMed: 19644473]

Lock R, Roy S, Kenific CM, Su JS, Salas E, Ronen SM, Debnath J. Autophagy facilitates glycolysis during Ras-mediated oncogenic transformation. Mol Biol Cell. 2011; 22:165–178. [PubMed: 21119005]

Lozy F, Karantza V. Autophagy and cancer cell metabolism. Semin Cell Dev Biol. 2012; 23:395–401. [PubMed: 22281437]

Luo J, Manning BD, Cantley LC. Targeting the PI3K-Akt pathway in human cancer: rationale and promise. Cancer Cell. 2003; 4:257–262. [PubMed: 14585353]

Mitra K. Mitochondrial fission-fusion as an emerging key regulator of cell proliferation and differentiation. Bioessays. 2013; 35:955–964. [PubMed: 23943303]

Mitra K, Wunder C, Roysam B, Lin G, Lippincott-Schwartz J. A hyperfused mitochondrial state achieved at G1-S regulates cyclin E buildup and entry into S phase. Proc Natl Acad Sci USA. 2009; 106:11960–11965. [PubMed: 19617534]

Author Manuscript Author Manuscript Author Manuscript Author Manuscript

Montagut C, Settleman J. Targeting the RAF-MEK-ERK pathway in cancer therapy. Cancer Letters. 2009; 283:125–134. [PubMed: 19217204]

Moore PS, Sipos B, Orlandini S, Sorio C, Real FX, Lemoine NR, Gress T, Bassi C, Klöppel G, Kalthoff H, et al. Genetic profile of 22 pancreatic carcinoma cell lines. Analysis of K-ras, p53, p16 and DPC4/Smad4. Virchows Arch. 2001; 439:798–802. [PubMed: 11787853]

Pitts KR, McNiven MA, Yoon Y. Mitochondria-specific function of the dynamin family protein DLP1 is mediated by its C-terminal domains. J Biol Chem. 2004; 279:50286–50294. [PubMed: 15364948]

Qian W, Choi S, Gibson GA, Watkins SC, Bakkenist CJ, Houten BV. Mitochondrial hyperfusion induced by loss of the fission protein Drp1 causes ATM-dependent G2/M arrest and aneuploidy through DNA replication stress. J Cell Sci. 2012; 125:5745–5757. [PubMed: 23015593]

Qian W, Wang J, Van Houten B. The role of dynamin-related protein 1 in cancer growth: a promising therapeutic target? Expert Opin Ther Targets. 2013; 17:997–1001. [PubMed: 23888838]

Rao S, Tortola L, Perlot T, Wirnsberger G, Novatchkova M, Nitsch R, Sykacek P, Frank L, Schramek D, Komnenovic V, et al. A dual role for autophagy in a murine model of lung cancer. Nature Communications. 2014; 5:3056.

Rehman J, Zhang HJ, Toth PT, Zhang Y, Marsboom G, Hong Z, Salgia R, Husain AN, Wietholt C, Archer SL. Inhibition of mitochondrial fission prevents cell cycle progression in lung cancer. Faseb J. 2012; 26:2175–2186. [PubMed: 22321727]

Rosenfeldt MT, Ryan KM. The multiple roles of autophagy in cancer. Carcinogenesis. 2011; 32:955–963. [PubMed: 21317301]

Rosenfeldt MT, O'Prey J, Morton JP, Nixon C, MacKay G, Mrowinska A, Au A, Rai TS, Zheng L, Ridgway R, et al. p53 status determines the role of autophagy in pancreatic tumour development. Nature. 2013; 504:296–300. [PubMed: 24305049]

Sebolt-Leopold JS, Herrera R. Targeting the mitogen-activated protein kinase cascade to treat cancer. Nat Rev Cancer. 2004; 4:937–947. [PubMed: 15573115]

Sheridan C, Martin SJ. Mitochondrial fission/fusion dynamics and apoptosis. Mitochondrion. 2010; 10:640–648. [PubMed: 20727425]

Shields JM, Pruitt K, McFall A, Shaub A, Der CJ. Understanding Ras: 'it ain't over 'til it's over'. Trends Cell Biol. 2000; 10:147–154. [PubMed: 10740269]

Son J, Lyssiotis CA, Ying H, Wang X, Hua S, Ligorio M, Perera RM, Ferrone CR, Mullarky E, Shyh-Chang N, et al. Glutamine supports pancreatic cancer growth through a KRAS-regulated metabolic pathway. Nature. 2013; 496:101–105. [PubMed: 23535601]

Stanton VP, Nichols DW, Laudano AP, Cooper GM. Definition of the human raf amino-terminal regulatory region by deletion mutagenesis. Mol Cell Biol. 1989; 9:639–647. [PubMed: 2710120]

Stokes JB, Adair SJ, Slack-Davis JK, Walters DM, Tilghman RW, Hershey ED, Lowrey B, Thomas KS, Bouton AH, Hwang RF, et al. Inhibition of Focal Adhesion Kinase by PF-562,271 Inhibits the Growth and Metastasis of Pancreatic Cancer Concomitant with Altering the Tumor Microenvironment. Mol Cancer Ther. 2011; 10:2135–2145. [PubMed: 21903606]

Strohecker AM, Guo JY, Karsli-Uzunbas G, Price SM, Chen GJ, Mathew R, McMahon M, White E. Autophagy sustains mitochondrial glutamine metabolism and growth of BrafV600E-driven lung tumors. Cancer Discovery. 2013; 3:1272–1285. [PubMed: 23965987]

Su B, Wang X, Bonda D, Perry G, Smith M, Zhu X. Abnormal mitochondrial dynamics–a novel therapeutic target for Alzheimer's disease? Mol Neurobiol. 2010; 41:87–96. [PubMed: 20101529]

Taguchi N, Ishihara N, Jofuku A, Oka T, Mihara K. Mitotic phosphorylation of dynamin-related GTPase Drp1 participates in mitochondrial fission. J Biol Chem. 2007; 282:11521–11529. [PubMed: 17301055]

Ushio-Fukai M, Nakamura Y. Reactive oxygen species and angiogenesis: NADPH oxidase as target for cancer therapy. Cancer Letters. 2008; 266:37–52. [PubMed: 18406051]

Vander Heiden MG, Cantley LC, Thompson CB. Understanding the Warburg effect: the metabolic requirements of cell proliferation. Science. 2009; 324:1029–1033. [PubMed: 19460998]

Warburg O. On the origin of cancer cells. Science. 1956; 123:309–314. [PubMed: 13298683]

Westermann B. Mitochondrial fusion and fission in cell life and death. Nat Rev Mol Cell Biol. 2010; 11:872–884. [PubMed: 21102612]

Author Manuscript Author Manuscript Author Manuscript Author Manuscript

Xia C, Meng Q, Liu LZ, Rojanasakul Y, Wang XR, Jiang BH. Reactive oxygen species regulate angiogenesis and tumor growth through vascular endothelial growth factor. Cancer Res. 2007; 67:10823–10830. [PubMed: 18006827]

Yoon Y, Galloway CA, Jhun BS, Yu T. Mitochondrial dynamics in diabetes. Antioxid Redox Sign. 2011; 14:439–457.

Youle RJ, Karbowski M. Mitochondrial fission in apoptosis. Nat Rev Mol Cell Biol. 2005; 6:657–663. [PubMed: 16025099]

Yu T, Jhun BS, Yoon Y. High-glucose stimulation increases reactive oxygen species production through the calcium and mitogen-activated protein kinase-mediated activation of mitochondrial fission. Antioxid Redox Sign. 2011; 14:425–437.

Zhang GE, Jin HL, Lin XK, Chen C, Liu XS, Zhang Q, Yu JR. Anti-tumor effects of mfn2 in gastric cancer. Int J Mol Sci. 2013; 14:13005–13021. [PubMed: 23797661]

Zhao J, Zhang J, Yu M, Xie Y, Huang Y, Wolff DW, Abel PW, Tu Y. Mitochondrial dynamics regulates migration and invasion of breast cancer cells. Oncogene. 2013; 32:4814–4824. [PubMed: 23128392]

Author Manuscript
Author Manuscript
Author Manuscript
Author Manuscript

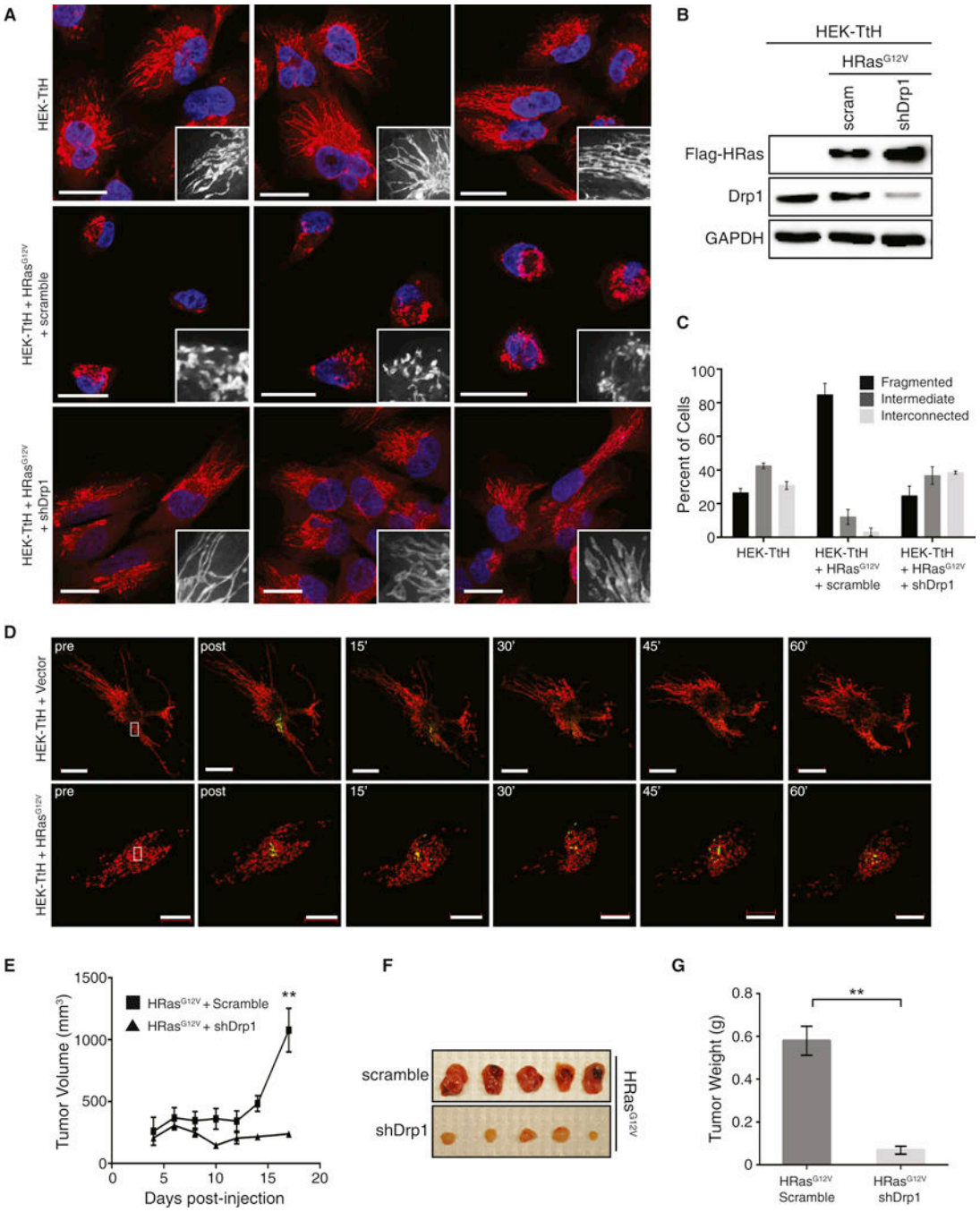

Figure 1. Ras-induced mitochondrial fission is required for tumor growth

(A) Mitochondrial morphologies of HEK-TtH cells or HEK-TtH cells stably expressing $HRas^{G12V}$ plus scramble or Drp1 shRNA. Red: MitoTracker Red; Blue: DAPI. Scale Bar = 20μm. (B) Immunoblot of Flag-$HRas^{G12V}$ and Drp1 in cells visualized in (A). GAPDH = Loading control. (C) Quantitation of mitochondrial morphologies observed in cells described in (A). n>50 cells, blindly scored by 3 people, 3 independent experiments; Error bar: S.E.M of mean percentages from 1 representative experiment. (D) HEK-TtH cells expressing vector or $HRas^{G12V}$ were transfected with mito-dsRed and mito-PA-GFP. mito-

Author Manuscript Author Manuscript Author Manuscript Author Manuscript

PA-GFP was activated by a 405-nm laser pulse in a 4μm region of interest (white box) then green fluorescence was tracked over a 1 hour time course. (E–G) HEK-TtH cell expressing $HRas^{G12V}$ and an shRNA targeting either scramble control or Drp1 were injected into mice and tumor volume (E) was measured over time. Tumors were removed at day 17 to be photographed (F) and weighed (G). n=5 tumors per cell line; error bars: S.E.M. of mean tumor volume (E) or tumor weight (G). ** Two-tailed student t-test, p=0.00749 (E) or p=0.00242 (G).

Author Manuscript Author Manuscript Author Manuscript Author Manuscript

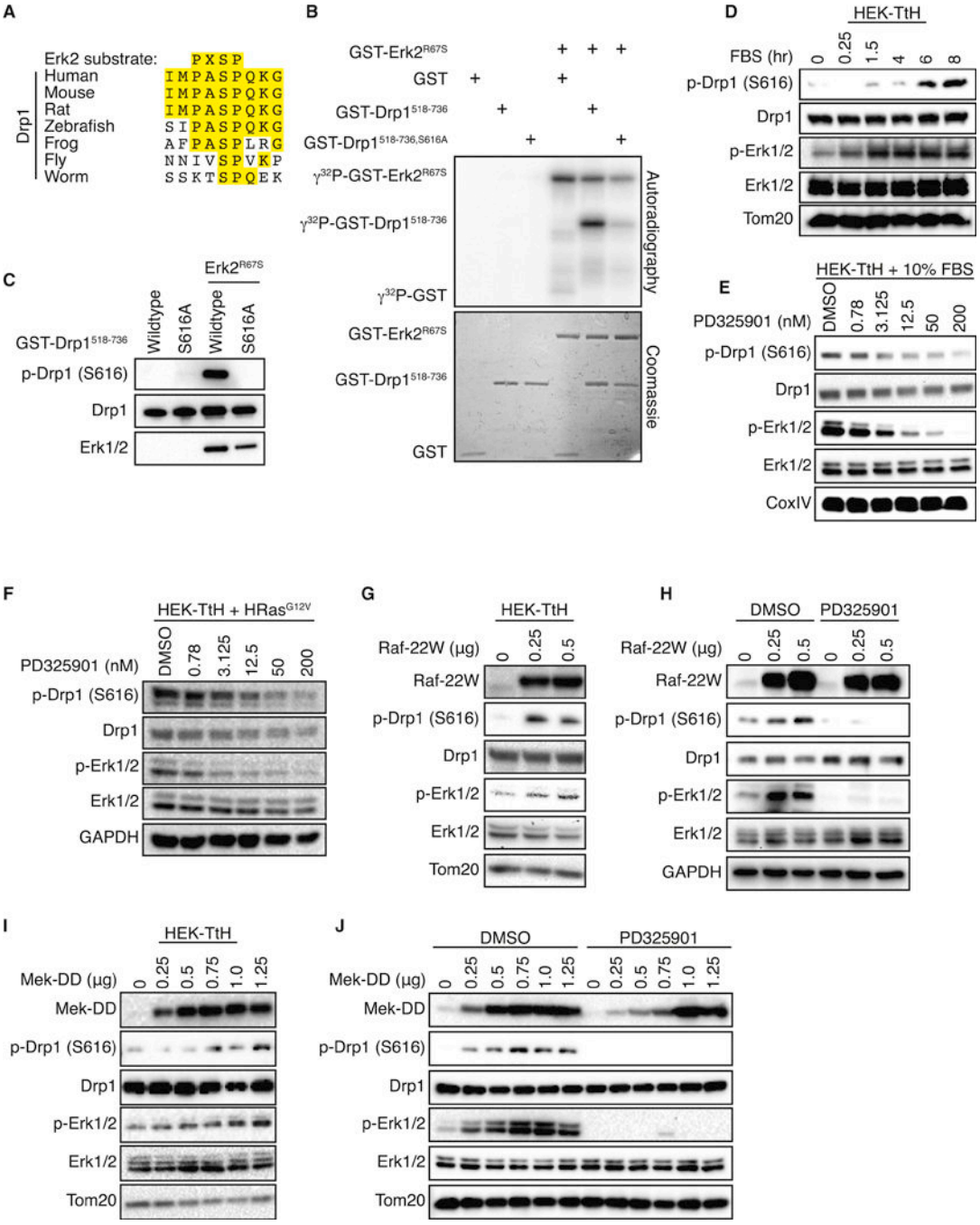

Figure 2. Erk2 phosphorylates Drp1 Serine 616

(A) Alignment of the consensus Erk2 target sequence with amino acids 612–620 of human Drp1 (isoform 1) and the corresponding sequence from the indicated species. (B–C) Recombinant, active GST-Erk2^{R67S} was incubated with either GST alone, GST-Drp1$^{518–736}$ or GST-Drp1$^{518–736,\ S616A}$ in the presence of γ^{32}P-ATP (B) or ATP (C) and resolved by SDS-PAGE. Drp1 phosphorylation was detected by autoradiography (B) or immunoblot (A). (D–J) Phosphorylation of Drp1 (P616) and Erk1/2 (Y202/T204) were monitored by immunoblot in the following cells: (D) HEK-TtH cells grown in serum-free DMEM

Author Manuscript Author Manuscript Author Manuscript Author Manuscript

supplemented with 10μM Mek inhibitor PD325901 for 16 hrs, then supplemented with 10% FBS over an 8-hour time course; (E) HEK-TtH cells supplemented with 10% FBS and treated with 0.78–200nM of PD325901 for 8 hrs. (F) HEK-TtH cells stably expressing $HRas^{G12V}$ treated with 0.78–200nM of PD325901 for 8 hrs; (G) HEK-TtH cells transfected with increasing amounts of Raf-22W; (H) HeLa cells transfected with increasing amounts of Raf-22W in the presence of DMSO or PD325901; (I) HEK-TtH cells transfected with increasing amounts of MEK-DD; (J) HeLa cells transfected with increasing amounts of active MEK-DD in the presence of DMSO or PD325901; Tom20, CoxIV, GAPDH: Loading Controls.

Author Manuscript
Author Manuscript
Author Manuscript
Author Manuscript

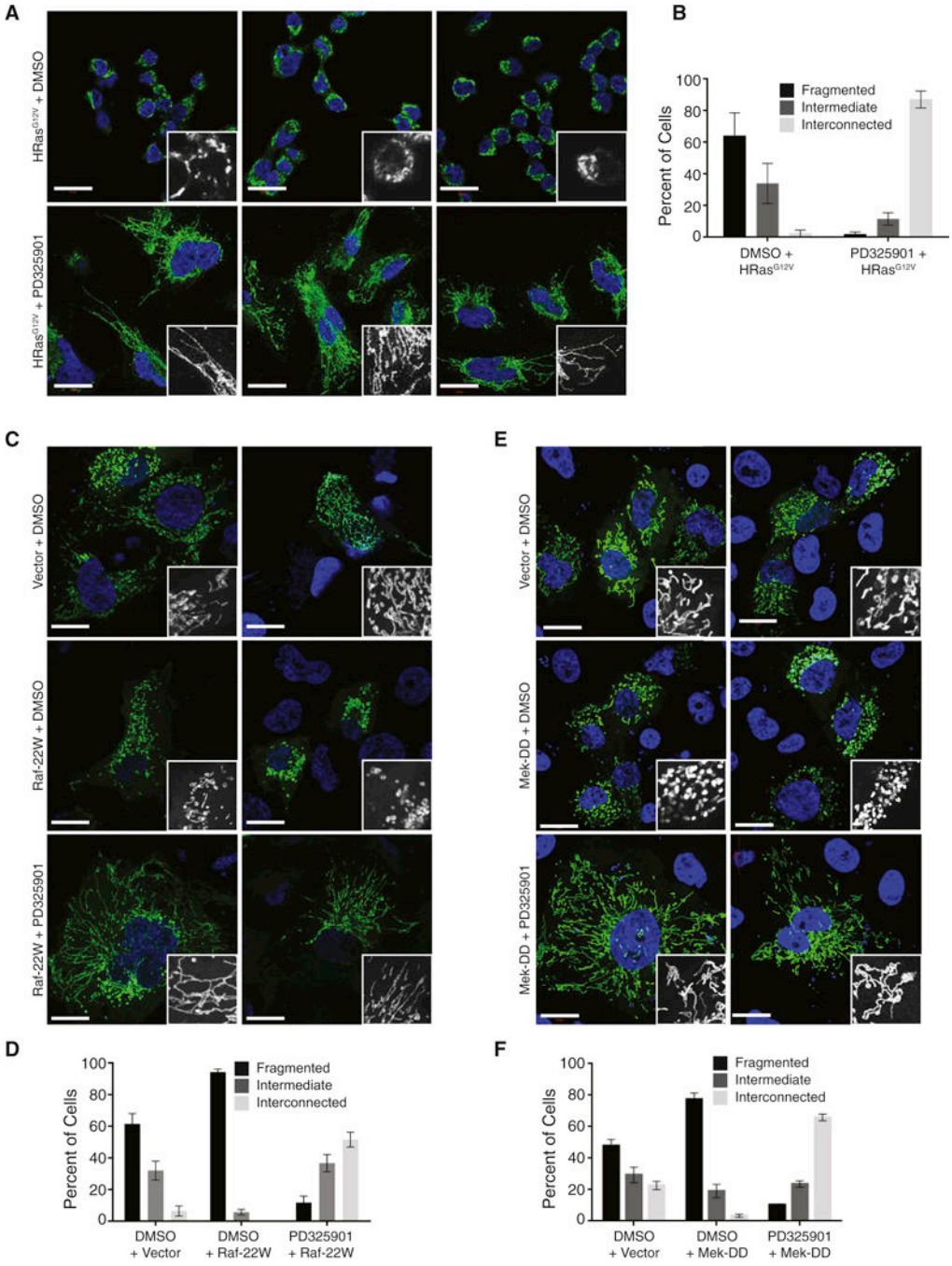

Figure 3. Activation of Ras or MAPK signaling leads to Mek-dependent mitochondrial fragmentation

(A) Mitochondrial morphologies of HEK-TtH cells stably expressing mito-YFP and HRas^{G12V} and treated with either DMSO or 200nM PD325901 for 24 hours. Green: mito-YFP; Blue: DAPI. Scale Bar = 20μm. (B) Quantitation of mitochondrial morphologies observed in cells described in (A). n>50 cells, blindly scored by 5 people, 3 independent experiments; Error bar: S.E.M of mean percentages from 1 representative experiment. (C–F) Mitochondrial morphologies of HEK-TtH cells transfected with mito-YFP plus either vector, Raf-22W or Mek-DD and treated with either DMSO or 200nM PD325901 for 24

hours as indicated. Green: mito-YFP; Blue: DAPI. Scale Bar = 20μm; Quantitation of mitochondrial morphologies: n>50 cells, blindly scored by 5 people, 3 independent experiments; Error bar: S.E.M of mean percentages from 1 representative experiment.

Author Manuscript Author Manuscript Author Manuscript Author Manuscript

Author Manuscript Author Manuscript Author Manuscript Author Manuscript

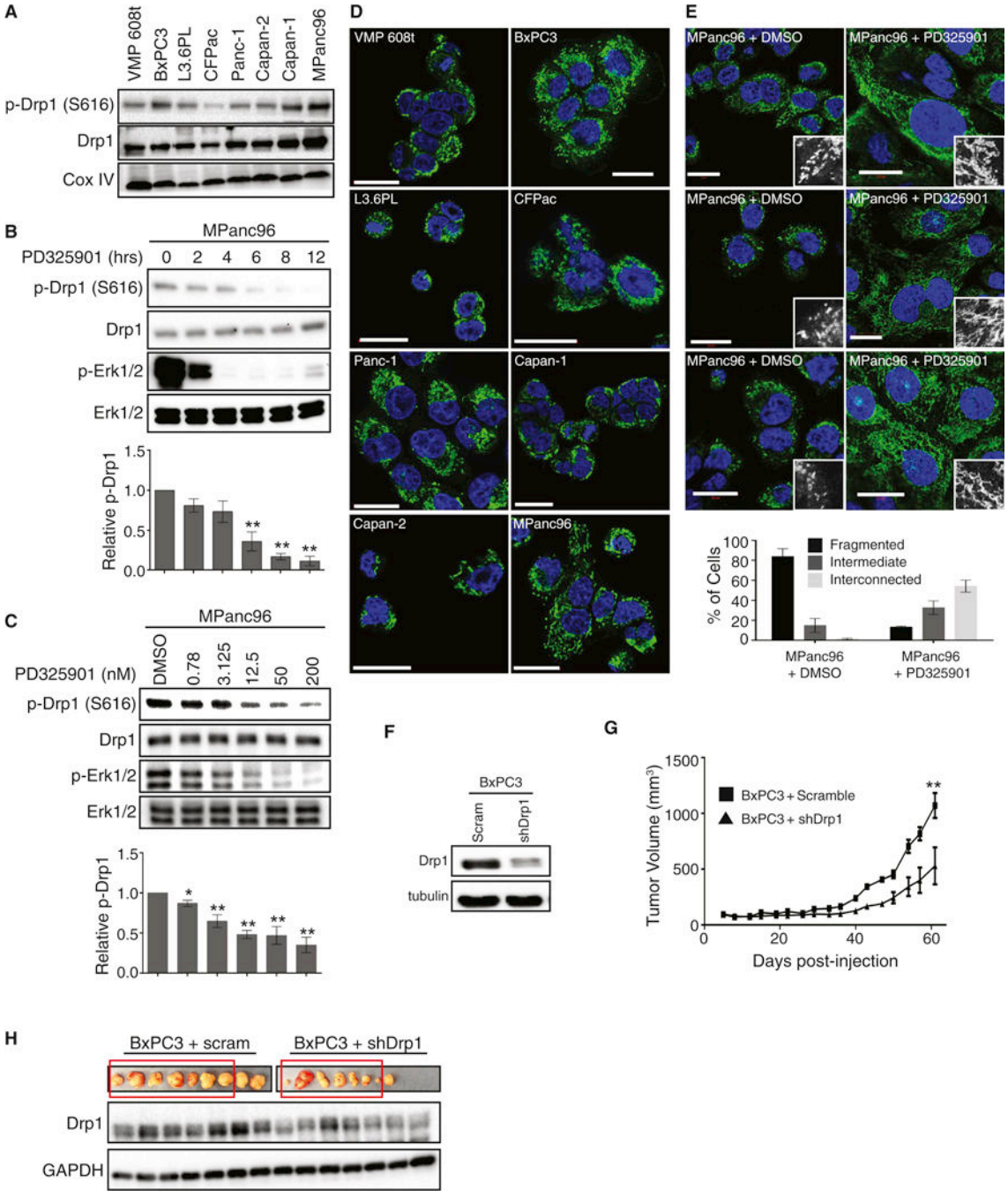

Figure 4. Patient-derived pancreatic cancer cell lines are characterized by Mek-dependent Drp1 phosphorylation and mitochondrial fragmentation

(A) Immunoblot analysis of phospho-Drp1 (P616) and Drp1 in a panel of 8 patient-derived pancreatic cell lines. CoxIV: Loading Control. (B–C) Immunoblot analysis of MPanc96 cells treated with 200nM PD325901 over a timecourse of 12 hours (C) or treated with 0.78–200nM for 8 hours (D). Graph: p-Drp1 levels normalized to total Drp1 levels; n=3, Error bars: S.E.M. Two-tailed student t-test comparing treatment to control, **p<0.01; *p<0.05. (D) Mitochondrial morphology of 8 patient-derived pancreatic cancer cell lines. Green: anti-Tom20; Blue: DAPI. Scale Bar = 20μm. (E) Mitochondrial morphology of MPanc96 cells

Author Manuscript Author Manuscript Author Manuscript Author Manuscript

treated with DMSO or 200nM PD325901 for 48hrs. Green: anti-Tom20; Blue: DAPI. Scale Bar = 20μm. Graph: quantitation of mitochondrial morphologies. n>50 cells, blindly scored by 5 people, 3 independent experiments; Error bar: S.E.M of mean percentages from 1 representative experiment. (F–H) BxPC3 cells expressing scramble or Drp1 shRNA were analyzed by immunoblot (F) then injected into mice and tumor volume was measured over time (G). Tumors were excised and analyzed by immunoblot (H). Blot represents first 7 tumors for each cell type (red boxes). Tubulin, GAPDH: Loading controls. Error bars: S.E.M. of mean tumor volume. ** Two-tailed student t-test, $p<0.004$.

Author Manuscript Author Manuscript Author Manuscript Author Manuscript

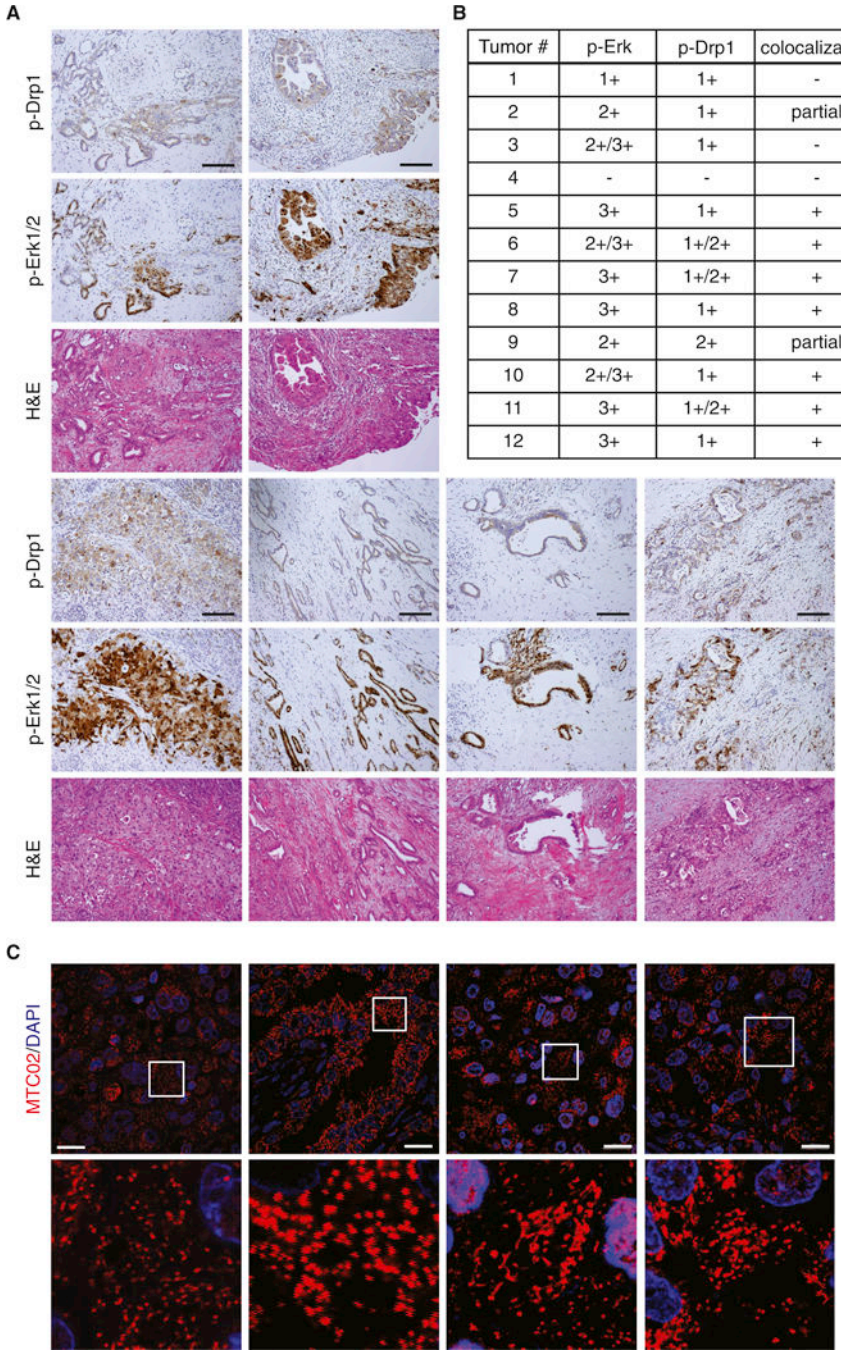

Tumor #	p-Erk	p-Drp1	colocalization
1	1+	1+	-
2	2+	1+	partial
3	2+/3+	1+	-
4	-	-	-
5	3+	1+	+
6	2+/3+	1+/2+	+
7	3+	1+/2+	+
8	3+	1+	+
9	2+	2+	partial
10	2+/3+	1+	+
11	3+	1+/2+	+
12	3+	1+	+

Figure 5. Drp1 S616 is phosphorylated in human pancreatic ductal adenocarcinoma

(A) Three serial sections were cut from formalin-fixed, paraffin-embedded sections from 12 pancreatic ductal adenocarcinomas and stained with Hematoxylin and Eosin (H&E) or antibodies against phospho-Drp1 (S616) and phospho-Erk1/2 (T202/Y204). Representative images of colocalization are shown from 6 tumors. Scale Bar = 100μm (IHC). (B) The levels of phospho-Drp1 (S616) and phospho-Erk1/2 (T202/Y204) staining, as well as the degree of co-localization, were determined for each of 12 pancreatic ductal adenocarcinomas examined. (C) Additional sections were cut from two of the tumors (7, 11) and stained with

an anti-mitochondria antibody (MTC02) to detect mitochondria (red). Blue: DAPI. Scale Bar = 20μm.

Author Manuscript Author Manuscript Author Manuscript Author Manuscript

Author Manuscript Author Manuscript Author Manuscript Author Manuscript

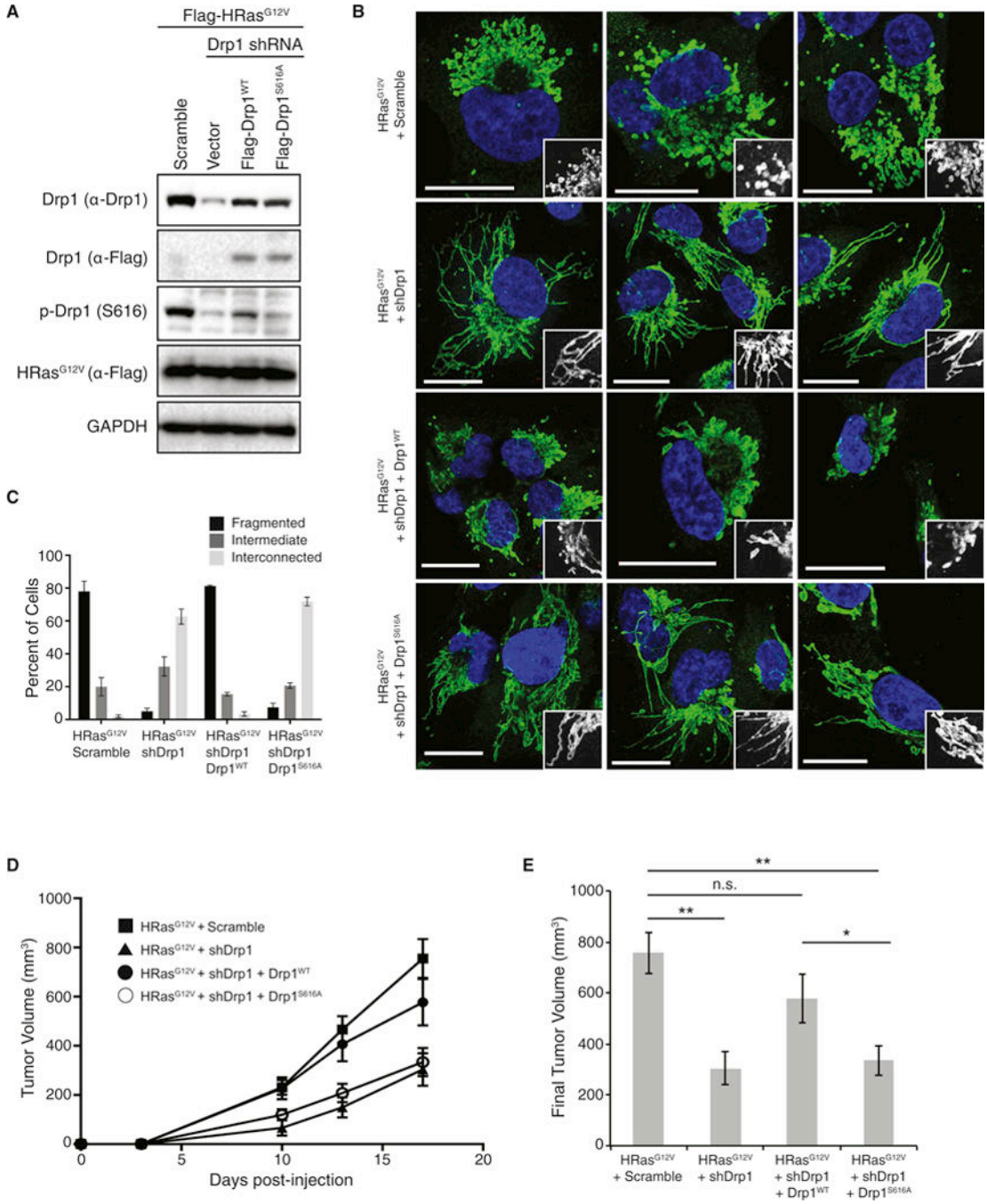

Figure 6. Drp1 Serine 616 is required for Ras-induced mitochondrial fission and Ras-induced tumor growth

(A) HEK-TtH cells were engineered to express Flag-HRas^{G12V} plus an shRNA targeting either scramble or Drp1 and rescued with either vector, Flag-Drp1^{WT} or Flag-Drp1^{S616A}. (B) The mitochondrial morphologies were analyzed. Green: anti-Tom20; Blue: DAPI. (C) Mitochondrial morphologies were quantified in: n>50 cells, blindly scored by 5 people, 3 independent experiments; Error bar: S.E.M of mean percentages from 1 representative experiment. Scale Bar = 20μm. (D–E) Cells were injected into mice and tumor volume measured over time (D). Tumor volumes at day 17 are shown in (E). n=10 tumors per cell

line; error bar: S.E.M. of mean tumor volume. Two-tailed student t-test, **p<0.001; *p<0.05; n.s.=p>0.15.

Author Manuscript Author Manuscript Author Manuscript Author Manuscript